International Journal for Innovative Engineering and Management Research

A Peer Revieved Open Access International Journal

www.ijiemr.org

IJIEMR Transactions, online available on 4th Sept 2019. Link :http://www.ijiemr.org/downloads.php?vol=Volume-08&issue=ISSUE-09

Title **PV MODULE INTEGRATED CONVERTER IRRADIANCE-ADAPTIVE FOR HIGH EFFICIENCY OF POWER QUALITY IN STANDALONES AND DC MICRO GRID APPLICATIONS**

Volume 08, Issue 09, Pages: 337–352.

Paper Authors

V ASHOK, G DEEPAK KUMAR, G HARISH

Anu Bose Institute of Technology K.S.P Road, New paloncha, Bhadradri Kothagudem, Telangana, India

International Journal for Innovative Engineering and Management Research
A Peer Revieved Open Access International Journal
www.ijiemr.org

PV MODULE INTEGRATED CONVERTER IRRADIANCE-ADAPTIVE FOR HIGH EFFICIENCY OF POWER QUALITY IN STANDALONES AND DC MICRO GRID APPLICATIONS

V ASHOK[1], G DEEPAK KUMAR[2], G HARISH[3]
[1]Assistant prof., [2,3]UG Students
[1,2,3]Dept. of Electrical and Electronics Engineering, Anu Bose Institute of Technology K.S.P Road, New paloncha, Bhadradri Kothagudem, Telangana, India.
ashok206402@gmail.com[1], deepakgokavapu@gmail.com[2], harishgadida@gmail.com[3]

Abstract:- The take a stab at proficient and practical photovoltaic frameworks persuaded the power electronic plan created here. Thework brought about a DC-DC converter formodule combination and conveyed most extreme powerpoint following (MPPT) withanovel versatile control conspire. The last is fundamental forthe joined highlights of high vitality effectiveness and highpowerquality overawide scope of working conditions. The exchanging recurrence is ideally tweaked as an element of sunlight based irradianceforpower change effectiveness boost. With the ascent of irradiance, the recurrence is decreased to arrive at the transformation productivity target. A hunt calculation is created to decide the ideal exchanging recurrence step. Decreasing of exchanging recurrence may, in any case, bargain MPPT productivity. Besides, it prompts expanded swell substance. Consequently, to accomplish a uniform highpowerquality at all conditions, interleaved convertercellsare adaptively enacted. The general expense iskeptlow by choosing parts that take into account executing the capacities with ease. Reenactment results demonstrate the high estimation of the module incorporated converter for DC independent and microgrid applications. A 400 W model was actualized at 0.14 Euro/W. Testing indicated efficienciesabove95% considering misfortunes from influence transformation, MPPT, and estimation andcontrol hardware.

Index Terms:-Boost Converter, DistributedMaximum PowerPointTracking (DMPPT), micro grid, module integrated converter (MIC), Photovoltaics(PV), PowerOptimizer, PowerQuality, SolarIrradiance, SwitchingFrequencyModulation(SFM).

I. INTRODUCTION

SOLAR vitality transformation through photovoltaics (PV) isa quickly developing wellspring of greenpowersupply [1]. Improving the proficiency ofPV frameworks is broadly observed as significant in supporting this pattern [2], [3]. This worries the improvement ofthePV cells, yet in addition ofthe power electronic circuits and controls associated with them. Past the PVcells, the general PV framework proficiency is incredibly influenced bythree elements. Right off the bat, it is influenced by the granularity level of dispersed most extreme powerpoint following (DMPPT)

[2], [4]–[6]. Besides, itis affected by the exactness and speedofthe used MPPT calculation [7]. Thepower change proficiency ofthe utilized converter topology assumes akey job [3],[8],[9]. With respect to initially factor modulecoordinatedconverters (MIC) or power enhancers speaking to module-level DMPPT exceptionally improve PVpower gathering productivity [3][9][11]. As for the subsequent factor, late researchhas considered utilizing different converter topologies andnovel MPPT calculations inside MICs for PV framework effectiveness expansion [8],[10]. Buck and lift as essential non-confined powerconverters are generally utilized in MICs[3][9][11]. In this unique situation, the power transformation proficiency ofthe MIC topology asa third factor is profoundly affected bythe used balance plot [9][12][14]. Exchanging recurrence adjustment (SFM) is a type heartbeat widthtweak (PWM) using numerous exchanging frequencies incontrolling DC-DC converters [12][15][17]. The SFM hasbeen utilized forthe accompanying applications. Ithas added tothe decrease of electromagnetic impedance (EMI) discharge bypower range spreading [18]–[20]. In [21], SFM was used for electrical cable correspondence in DC microgrids, where all power converters share a typical DC transport. Limiting yield current complete consonant twisting in current source invertersthrough a SFM plan was presented in [22]. What's more, SFM hasimproved the vigor tothe varieties of reverberation parameters & information voltagesin current source parallel full converters[23]. Likewise, SFM has been utilized for burden subordinate advancement of intensity change proficiency at any conduction mode [15]–[17]. The fruitful utilization of SFM in burden subordinate streamlining recommends that it might likewise be an alluring competitor when age intensely changes. Such a circumstance is experienced in the sun based power reaping of MICs. This perception has roused the work for this paper to explore the commitment of the SFM to further improve the PV framework productivity past the three elements examined previously. In the logical writing, just fixed exchanging frequencies havebeen accounted for in the control ofthe MICs[3][5]. Thefixed exchanging recurrence was chosen to keep up the MIC atall examined irradiancelevels. Subsequently, a persistent power stream was accomplished, and the reaped powerfrom the PVsource was expanded [14]. In any case, the choice of a fixed exchanging recurrence includes an exchange off. A higher exchanging recurrence decreases the power change proficiency because of exchanging misfortunes. Itisthe primary commitment ofthispaper to plan an irradiance-adjusted SFM plot forMICs to advance the MIC productivity atall irradiancelevels. Along these lines, the general vitality collected throu the PV framework isimproved. A tale stepwise strategy withan incorporated mechanized pursuit calculation to decide the number and estimations ofthe ideal exchanging frequencies oftheSFM dependent onthe irradiance created. Alluring component is uniform powerquality. Accomplishing a uniform powerquality is testing A SFM adjusts the exchanging recurrence. Asa potential arrangement, interleavedconverters show high capacity of adjusting the yield swell [24][25]. Besides, theycan improve proficiency and diminish EMI[24][27]. Handling thenonuniform swell substance coming about because of SFM hasnotbeen tended to sofar in the logical writing. As an integral commitment tothe

International Journal for Innovative Engineering and Management Research
A Peer Revieved Open Access International Journal
www.ijiemr.org

irradianceadaptive SFM, the proper number ofcellsfor a versatile converter topology andthe relating actuation times in connection totheSFM plan are created. This has the result of diminished swell substance andEMI discharge. The above cases of productivity, yield swell, and EMI are substantiated by physical usage and testing oftheMIC. The performed examinations secured independent andDCmicrogrid applications. Followingthis presentation, the versatile SFM plan and MIC topology for PV applications is exhibited in Section II. Besides, the blend with a quick responding MPPT is shown. In Section III, issues of DC microgrid joining are tended to. Reproduction results and test approval are exhibited in SectionsIV,V, separately. Ends are attracted SectionVI. Furthermore, the acknowledgment ofthe MIC with ease is expounded uponin theAppendix.

II. PV-ADAPTED SWITCHING FREQUENCY MODULATION

Using perfect SFM in PVsystems is exhibited inthree rule parts:the irradiance-flexible SFM; the improvement ofthe SFM plan and MICtopology; and theMPPT estimation.

A. Irradiance-adaptive SFM

The PVcurrent increments quality withthe sun powered irradiance. Athigh irradiance, thePV-bolstered MICcan work in CCM forawide burden extend. Low exchanging frequencies all things considered can add toahigh effectiveness without adjusting theconverter method of activity to intermittent conduction mode (DCM). The immediate power drawn from information sources iszero exactly when the inductor current iszero inDCM [14]. Expanding the exchanging recurrence cankeep activity inCCM. Consequently,

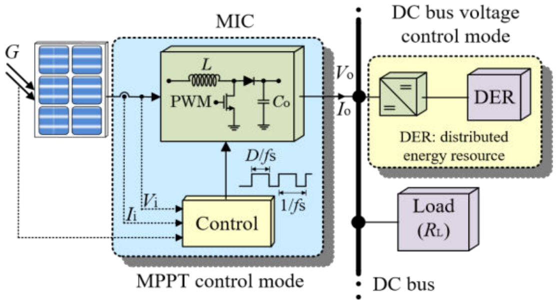

Fig. 1. PV module coordinated converterin DC microgridapplication.

exchanging recurrence fs isproposed to be adaptively controlled withthe sun based irradiance Gas a contribution:

$$f_s = \begin{cases} f_{s0} = f_{smax}, & G_0 \leqslant G < G_1 \\ f_{si} = f_{s(i-1)} - \Delta f_{si}, & 1 \leqslant i \leqslant n, G_i \leqslant G < G_{i+1} \end{cases}, \quad (1)$$

where I isthe counter ofdiscrete exchanging recurrence f_{si}; f_{smax} is the most extreme exchanging recurrence speaking to f_{si} for I = 0; Δf_{si} indicates the recurrence variety step I; G0 and Gn+1 are the base and greatest irradiances considered, separately; Gi for I = 1, 2, . . ., n arethe moderate irradiance edges. Steady of Δfs, (1) lessens to:

$$f_{si} = f_{smax} - i \cdot \Delta f_s, \qquad 0 \leqslant i \leqslant n. \quad (2)$$

To distinguish the base exchanging recurrence for CCM activity of theMIC, eq. (16) of AppendixA relating fs, PWM obligation proportion D, and PVmodule relentless state normal voltageV_i andcurrent I_i modified as pursues:

$$f_s \geq \frac{D \cdot V_i}{2 \cdot I_i \cdot L}. \quad (3)$$

The obligation proportion D fora lift converterof proficiency η is approximated by[28]:

$$D = 1 - \frac{\eta \cdot V_i}{V_o}, \quad (4)$$

where V_o is the unfaltering state normal yield voltage of theMIC. In Fig. 1, theMIC is demonstrated sustaining aDC transport of a small scale network. Insuchcases, V_o is the DC transport voltage. Inclusion of(4) into(3)yields:

$$f_s \geq \frac{V_i}{2 \cdot I_i \cdot L} \cdot \left(1 - \frac{\eta \cdot V_i}{V_o}\right). \quad (5)$$

Forthe investigation of independent applications, theMIC is accepted to straightforwardly supplya heap withno otherDER control. Thus, an unadulterated resistive burden R_L, V_o is given by:

$$V_o = \sqrt{\eta \cdot V_i \cdot I_i \cdot R_L}. \quad (6)$$

Through (5) and (6), the base limit of the exchanging recurrence for CCM activity in independent application is assessed as pursues:

$$f_s \geq \frac{V_i}{2 \cdot I_i \cdot L} \cdot \left(1 - \sqrt{\frac{\eta \cdot V_i}{I_i \cdot R_L}}\right). \quad (7)$$

B. Optimization ofSFM Scheme and MICTopology

1) SFM Scheme Parameters: TheSFM conspire parameters spread the accompanying amounts: the base exchanging recurrence fsmin, the greatest exchanging recurrence fsmax, the recurrence steps Δfsi, and the irradiance edges Gi. The ideal estimation of the recurrence step and MICtopology forhigh effectiveness and powerquality are resolved. More center is devoted tothe lift converter as a MICtopology forreasons expressed in SectionIII.

The SFM plot forthe buckconverter case is portrayed in AppendixB. The deduction of the parameters inthe accompanying advances applies tothe lift converter.

Step 1: The base exchanging recurrence f_{smin} determined here relates to the most noteworthy irradiance in (1). It is resolved dependent on two focuses on that identify with vitality effectiveness and yield voltage swell. High exchanging frequencies decrease the top to-crest yield voltage swell ΔV_{opp}:

$$\Delta V_{opp} = \frac{I_o \cdot D}{C_o \cdot f_s}, \quad (8)$$

where C_o isthe capacitance ofthe MIC yield capacitor, and Io isthe unfaltering state normal yield current ofthe MIC. In any case, higher exchanging frequencies decrease theMIC effectiveness because of exchanging misfortunes. The base utilized exchanging recurrence should in the mean time fulfill the state of CCM. In this way, the exchanging recurrence limit for CCM activity at various irradiances is resolved right off the bat. The estimations of Vi and Ii ofthe PVmodule atMPP under various irradiances G are embedded into (5)(7). An objective productivity η andthe most extreme burden obstruction RL if there should arise an occurrence of independent applicationsare utilized to get theCCM exchanging recurrence limit of the considered lift converter andthe broke down PVmodule. The direction acquired is delineated in Fig.2a speaking to the most pessimistic scenario over all functional working conditions. Thus, for different DC transport voltages Vo, the direction acquired for the microgridcase delineated inFig.2b.

A security edge for force toward helplessness inthe parameters was joined into the breaking point. Atthe most essential irradiance showed up in Fig. 2, the base trading repeat forCCM action is f_{smin} CCM. A last estimation of f_{smin} is gotten by furthermore includinga prerequisite for a perfect voltage swell despite the CCM confinement. The last a motivating force for f_{smin} cannotbe lower, yet maybe higher than f_{smin} CCM.Step 2: The most extreme exchanging recurrence f_{smax} is reliant onthe limit of working the converter inCCM atthe least irradiance. From Fig. 2, thelower furthest reaches ofthe greatest exchanging recurrence atthe most minimal irradiance limit G0 canbe resolved. For insignificant exchanging misfortunes, estimations of fs at G0 in Fig.2is affirmed as f_{smax}. The choice of a low f_{smax} additionally keeps the range (f_{smax} $-f_{smin}$) rathertight. As found in [17], such a tight rangecan lessen negative impacts onthe stage edge and the hybrid recurrence ofthe converter control.

Step 3: Inthis progression, the exchanging recurrence step Δf_{smin} that relates tothe base noticeable irradiancechange ΔG_{min} is processed. From viewpoint, huge estimations of Δf_s lessen fs quicker and add to diminishing the converter

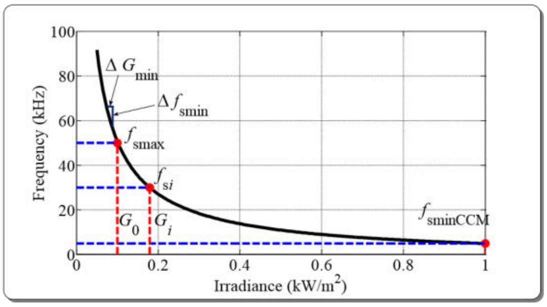

(a)

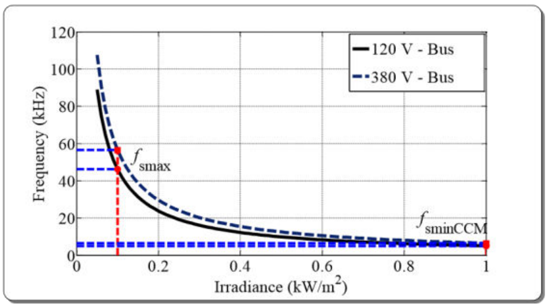

(b)

Fig. 2. Direction of the exchanging recurrence limit for working lift converter inCCM at various irradiance levelsfor: (an) independent case utilizing (7); (b) microgridcase utilizing (5).

control misfortune. In any case, the CCM activity condition might be disregarded. Then again, when choosing a certain Δfs, at that point thereisa relating ΔG when followingthe direction of Fig.2. Hence, a lower limit Δf_{smin} canbeset for fulfilling the limitation of ΔG_{min} whilefollowingthe direction. Inwhat pursues a declaration of Δfs as far as ΔG is inferred, and after that Δf_{smin} is assessed. As the sunlight based irradiance G strongly affects the converter inputcurrent, the pace of progress ofthe exchanging recurrence in (3) as for the converter inputcurrent isof intrigue. The adjustment in Vi with a little variety of Ii is thought tobe immaterial around theMPP. It will likewise be expected thatthe adjustment inthe obligation proportion D of the computerized controller because of a little change in Ii is not as much as its base advance ΔD and in this way D is viewed as unaltered. Thus, separating fs concerning Ii yields:

$$\frac{\mathrm{d}f_s}{\mathrm{d}I_i} \geq \frac{-D \cdot V_i}{2 \cdot I_i^2 \cdot L}. \quad (9)$$

According to (2), a $\Delta f_s > 0$ reduces f_s. Approximating in (9) $-\Delta f_s = \mathrm{d}f_s$ and $\Delta I_i = \mathrm{d}I_i$ gives:

$$\Delta f_s \leq \frac{D \cdot V_i}{2 \cdot I_i^2 \cdot L} \cdot \Delta I_i, \quad (10)$$

$$\Delta f_{smin} = \frac{D \cdot V_i \cdot K}{2 \cdot I_i^2 \cdot L} \cdot \Delta G_{min}, \quad (11)$$

$$K = \frac{\Delta I_i}{\Delta G}. \quad (12)$$

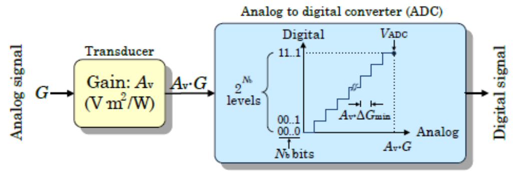

Fig. 3. Discretization ofthe irradiance for the SFMschemecontrol.

The base change in G thatcanbe detected by the simple to computerized converter (ADC) ofthecontrol chip ΔG_{min} is:

$$\Delta G_{min} = \frac{V_{ADC}}{2^{N_b} \cdot A_v}, \quad (13)$$

where VADC isthe greatest voltage thatcan be detected by theADC, Nb is the quantity of ADC bits, Av isthe utilized irradiance detecting gain. Since the slant ofthe bend in Fig.2 diminishes withthe expansion of G, the most extreme estimation of Δf_{smin} is hence acquired atthe least irradiance. Itis critical note of that Δfs is chosen sole then ΔG is resolved. At the point when Δfs is then set higher than Δf_{smin}, at that point ΔG is likewise bigger than ΔG_{min}, giving a doable handy usage.

International Journal for Innovative Engineering and Management Research
A Peer Revieved Open Access International Journal
www.ijiemr.org

Stage 4: The utilized exchanging recurrence step Δfs is resolved inthis progression. A fixed recurrence stepis accepted asin(2). In this manner, the recurrence step Δfs and the quantity utilized frequencies n+1 was connected :

$$\Delta f_s = \frac{f_{smax} - f_{smin}}{n}. \qquad (14)$$

The exchanging recurrence step must be more noteworthy than Δf_{smin} in (11). Sincea fixed recurrence stepis used, Δf_{smin} is determined atthe most reduced irradiance where itisat its greatest. In the mean time, a number estimation of Δfs is utilized for pragmatic execution.

A looking calculation for Δfs under the referenced requirements is then performed. The calculation increases the number n and decides Δfs from (14). At that point, it figures the utilized exchanging frequencies f_{si} from (2) and their relating irradiance edges Gi as in Fig. 2. In the future, the calculation figures the comparing MIC control misfortune for the broke down irradiance extents utilizing (18), (19), (20), (21), (22), (23), and (24) of the Appendix A. The calculation stops when Δfs turns out to be not exactly Δf_{smin} or when the further normal decrease of the MIC control misfortune with expanded n is not exactly a specific functional cutoff. The acquired Δfs and set of Gi edges are held.

Step 5: A hysteresis oftheirradiance limits is presented in this progression. So as to keep away from an undesirable ricocheting or regular variety of the exchanging recurrence because of mistakes, for instance because of flying items or sensorblames, a hysteresis isproposedto supplement(1)&(2). Forthe instance of four exchanging frequencies, Fig.4 demonstrates the proposed variety ofthe exchanging recurrence withthe sun based

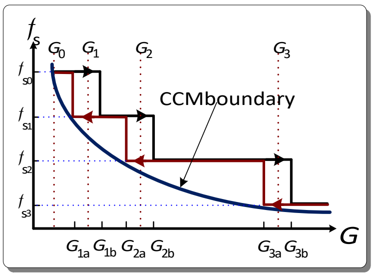

irradiance.

Fig. 4. Irradiance-based hysteresiscontrol of switchingfrequency.

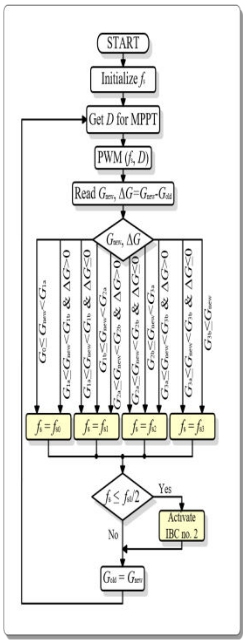

Fig. 5. Flow chartofadaptive MICcontrol scheme.

The dead groups are structured notto surpass the CCM limit as in Fig.4. The SFM control calculation is introduced in Fig.5 forfour exchanging frequencies. The calculation begins withthe most elevated exchanging recurrence, for activity in CCM. The obligation proportion Dis gotten from theMPPT calculation, and the PWMis refreshed. In view of the new irradiance estimation Gnew and the irradiancechange ΔG = Gnew −Gold, the exchanging recurrence is then refreshed, as well.

2) MICTopology: Combining a versatile MIC topology withthe streamlined SFM plan further adds tothe structure target of

International Journal for Innovative Engineering and Management Research
A Peer Revieved Open Access International Journal
www.ijiemr.org

keeping up abnormal state control quality. Without a versatile topology, So variety of the swell outcomes ina non-uniform power quality level overthe scope of fs utilized. For a practically uniform yield swell substance and lessEMI emanation at all frequencies, interleaved converter cellsare enacted as an element ofthe diminishing exchanging recurrence. Additionally, for the MPPT it is profitable thatthe information current swell drawn from the PVmodule is decreased

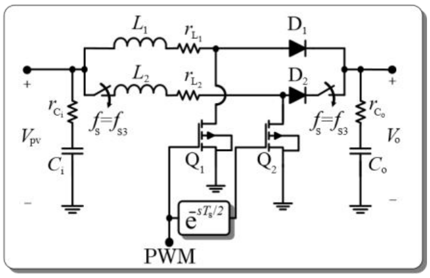

Fig. 6. Converter topology ofboost converter with interleavedcell activated at lowswitching frequency f_{s3}.

as well. The proposed numberof interleaved cells is the whole number truncation ofthe proportion fsmax/fsmin. In light of the utilized exchanging recurrence, the versatile control settles on the quantity ofinterleaved support converter cells (IBC) tobe initiated. The quantity of dynamic cells is settobe equivalent to j for exchanging frequencies not exactly or equivalent to fsmax/j. The convertertopology ofthe model with interleaved cells is appeared inFig.6. The second IBC is initiated at whatever point fs is not exactly fsmax/2, as likewise appeared in Fig. 5 where fsmax = fs0. For the given four discrete exchanging frequencies of the SFM, thisis the situation when fs = fs3. Because of the actuation, the EMI getsless and control quality stays high foraWide scope of delicate burdens [29], [30]. At low irradiance, thehigher exchanging recurrence improves the power quality, to the detriment of higher exchanging misfortunes. Actuating theIBC for this situation would prompt a moderately low improvementof an effectively decent power qualityat additional misfortunes. In this way, the IBC is just initiated at the low exchanging recurrence.

At low irradiance, exchanging misfortunes overwhelm conduction misfortunes and the other way around, as can be closed from (18)-(24) of AppendixA. At high irradiance, whenthe interleaved cellis actuated, the general misfortunes diminished in light of the fact that the conduction misfortune decrease surpasses the exchanging misfortune increment. Therefore, while improving force quality, control transformation proficiency destinations are completely bolstered by the versatile MIC topology, as well.

C. Most extreme PowerPointTracking

The Perturb and ObserveP&O calculation withthe base irritation stepsize for exact DMPPT is utilized. The MPPvoltage VMPP hypothetically lies somewhere in the range of 75% and 90% ofthe open circuit voltage Voc. Hence, the P&O calculation is intended to begin withan underlying obligation proportion comparing to 75% of Voc [31] to diminish the following time.

III. DC MICROGRID INTEGRATION

The adaptively controlled MIC is proposed for module level mix into the DC microgrid as appeared in Fig. 1. The information voltage of the MIC is balanced for MPPT, and the yield voltage is characterized by the DC transport voltage control units.

In this way, each PV-MIC mix goes about as a present source. In this way, the MIC is required to have info and yield evaluations reasonable for the basic PV modules and the transport voltage of the low-voltage DC microgrid, separately. A MIC yield voltage with low swell is in the mean time entirely alluring. As prominent voltages for DC microgrids, levels detailed incorporate 120 V, 170 V, 230 V, 340 V, and 380 V [32], [33]. Higher DC transport voltages require higher exchanging frequencies for keeping up CCM activity as finished up from Fig. 2b. Moreover, to venture up the ordinarily low PV module voltages, help converter topologies are required. The freewheeling diode of the lift converter can prevent any invert current from the DC transport thus secure the PV modules. In any case, there are additionally circumstances where buck converter topologies are fitting. Consequently, chose data for the buck case is given in Appendix B. On account of a lift converter, the suitable MIC input voltage run for DC microgrid incorporation is acquired from (4) by:

$$\frac{1-D_{\max}}{\eta}\cdot V_o < V_i < \frac{1-D_{\min}}{\eta}\cdot V_o, \qquad (15)$$

where D_{min} and D_{max} are the base and most extreme obligation proportions, individually. PV modules with MPP voltages abusing the lower furthest reaches of (15) are incorporated with converters having higher voltage gains [3]. PV modules damaging the furthest reaches of (15) would be incorporated utilizing buck converters.

IV. ANALYSIS BY SIMULATION

In this segment, the versatile topology and ideal SFM plan are broke down by reproduction. Parameters of the SFM plan are resolved in an initial step. At that point, recreation cases under factor irradiance examples are depicted for independent and DC microgrid cases. MATLAB/SIMULINKR was utilized to reenact the PV-MIC framework and the proposed control conspire. The converter circuit parts were intended to satisfy the targets of the MIC with information capacitance Ci of 220 μF, yield capacitance Co of 2200 μF, and inductances L1,2 of 0.5 mH. The mimicked PV module has a Voc of 44.8 V, VMPP of 36.5 V, cut off Isc of 5.5 An, and MPP current IMPP of 5.1 An at standard test conditions (STC). The parameters of the MPPT control calculation dependent on the used equipment are: least obligation proportion Dmin of 10%, most extreme obligation proportion Dmax of 90%, obligation proportion step ΔD of 0.4%, and 10 ADC bits as Nb.

A. SFM Scheme Parameters

The system of Section II-B1 was pursued to decide the SFM conspire parameters. In Step 1, a productivity higher than 97% and a yield voltage swell of 0.5% were focused on. The worth observed for fsmin was resolved to be 20 kHz, fulfilling the CCM condition spoken to by fsminCCM of Fig. 2. In Step 2, the most extreme exchanging recurrence fsmax was resolved. The most reduced examined irradiance G0 was proposed to be 0.1 kW/m2. From Fig. 2, a most extreme exchanging recurrence fsmax of around 50 kHz keeps the converter in CCM for a broke down burden extend from 0 kω to 3 kω For stage 3, ΔGmin was determined utilizing (13) with VADC of 5 V and Av of 0.005 V · m2/W. The parameter K is equivalent to 0.0051 A · m2/W. The most reduced irradiance G0 was utilized to get Δfsmin from (11). The estimations of Vi, Ii and D for the figuring of Δfsmin were 26.7 V, 0.5 An, and 0.8 separately. The calculation brought about an estimation of 429 Hz for Δfsmin comparing to a base distinguishable irradiance change ΔGmin of 0.98 W/m2. For Step 4, a whole number ideal estimation of 10 kHz for Δfs

International Journal for Innovative Engineering and Management Research
A Peer Revieved Open Access International Journal
www.ijiemr.org

was the result of the looking through calculation, and the quantity of frequencies was four. For estimations of n higher than 4, the decrease of the MIC control misfortune was not exactly a proposed handy utmost of 0.2%. The exchanging frequencies are at that point: 50 kHz, 40 kHz, 30 kHz, and 20 kHz. In view of Fig. 2, the comparing irradiance limits in kW/m2 were set to 0.1, 0.15, 0.2, and 0.35. In Step 5, a hysteresis dead band of 0.04 kW/m2 was chosen. In this way, G1a, G1b, G2a,G2b, G3a, and G3b as in Fig. 4 were doled out the accompanying qualities in kW/m2: 0.13, 0.17, 0.18, 0.22, 0.33, and 0.37.

The truncated whole number of the proportion fsmax/fsmin is equivalent to 2. Thusly, two lift converter cells were utilized in the MIC as appeared in Fig. 6. The second IBC is enacted at exchanging frequencies not exactly fsmax/2, so just at fs3.

B. Variable Irradiance Cases

In this subsection, the presentation of the PV-MIC framework for two sun oriented irradiance time arrangement following stepwise changing and persistently changing examples is talked about. To begin with, the presentation under a stepwise changing irradiance with four levels, 0.1 kW/m2, 0.175 kW/m2, 0.3 kW/m2, and 1 kW/m2, was investigated. The sunlight based irradiance, the exchanging recurrence, and the yield power are delineated in Fig. 7a. The MIC control had the option to differ the exchanging recurrence adaptively with the sun powered irradiance as per the SFM plot. In the mean time, the greatest PV power was productively followed. The converter was in CCM in the four cases. The interleaved converter cell is just actuated at the most noteworthy irradiance level at an exchanging recurrence of 20 kHz. This thusly diminishes the yield voltage swell from 1.30% to 0.59%. It is in a similar range with respect to the next irradiance levels. The impact of persistently changing irradiance designs on both the exchanging recurrence and the yield power is exhibited in Fig. 7b. The hysteresis engaged with the SFM of Fig. 4 can be seen as pursues. At the point when the irradiance rises and crosses 0.17 kW/m2 after 10.8 s into the recreation, the exchanging recurrence is diminished from 50 kHz to 40 kHz. Inverse way from 40 kHz to 50 kHz, this occurs at 0.13 kW/m2 after 49.7 s and falling irradiance. Comparable results are watched for the changes from 40 kHz to 30 kHz and from 30 kHz to 20 kHz.

In outline, the versatile topology and control plan demonstrates the normal following of various irradiance designs, modification of the exchanging recurrence for keeping up activity in CCM, and effective gathering of the greatest accessible power. Then, the yield voltage swell was kept at the ideal low levels by utilizing both the exchanging recurrence adjustment and the interleaved cell.

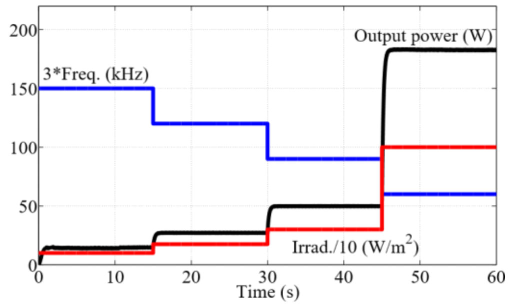

(a)

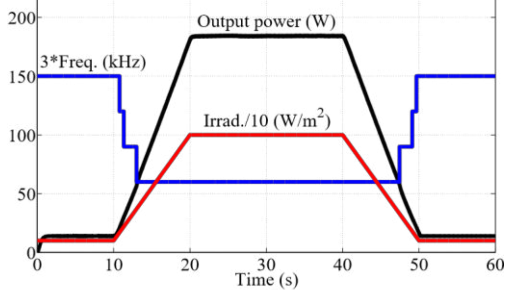

(b)

Fig. 7. Standalone case simulated irradiance, switching frequency, and power: (a) at step changing irradiance; (b) at continuously changing irradiance.

Table -I: Mic Components & Control Parameters

Component / Parameter	Value and properties
Input capacitor C_i	220 μF, 33 mΩ
Output capacitor C_o	2200 μF, 150 mΩ
Inductors $L_{1,2}$	500 μH, 85 mΩ
MOSFETs $Q_{1,2}$	150 V, 7.5 mΩ, FDP075N15A
Diodes $D_{1,2}$	180 V, 5 A, DSSK10-018A
PV module V_{oc}	44.8 V (STC)
PV module V_{MPP}	36.5 V (STC)
PV module I_{sc}	5.5 A (STC)
PV module I_{MPP}	5.1 A (STC)
Duty ratio limits $[D_{min}, D_{max}]$	[10 %, 90 %]
Duty ratio step ΔD	0.4 %
ADC bits and voltage	N_b = 10 bit, V_{ADC} = 5 V
Irradiance transducer gain	$A_v = 0.005\ V \cdot m^2/W$
Detectable irradiance change	$\Delta G_{min} = 0.98\ W/m^2$
Switching frequencies (kHz)	$f_{s0} = 50$, $f_{s1} = 40$, $f_{s2} = 30$, $f_{s3} = 20$
Irradiance boundaries (kW/m^2)	(0.13, 0.17), (0.18, 0.22), and (0.33, 0.37)
Interleaved converter cells	2, IBC is activated only at f_{s3}=20 kHz

V. EXPERIMENTAL SETUP AND VALIDATION

Here, the prototyping of the MIC and the preliminary course of action sought after by the introduction results are displayed. A 400 W model of the proposed MIC was made. With its data and yield voltage and current evaluations, the prototyped MIC is sensible for most by far of the typical PV modules and low voltage DC microgrid measures. The MIC of a volume of 800 cm3 and the test course of action are showed up in Fig. 8. The MIC sections and the parameters of the test course of action are recorded in Table I.

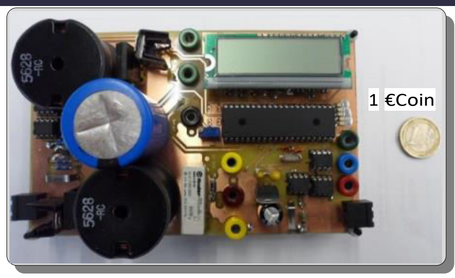

(a)

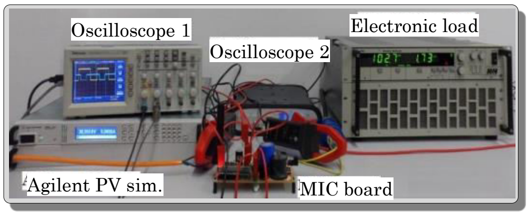

(b)

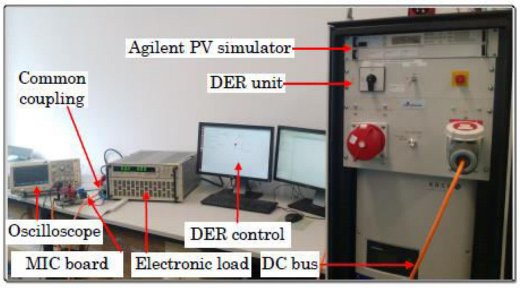

(c)

Fig. 8. (a) Module integrated converter MIC; (b) standalone experimental setup; (c) DC microgrid experimental setup.

A. Prototyping and Setup

1. **PV simulator:** The sun based exhibit test system Agilent E4361A was utilized to imitate the attributes of the contemplated PV module at different irradiance levels through its table mode. The voltage-current attributes of the examined module are provided in voltage ventures of 12 mV, which is the test system's base voltage step.
2. **Load:** An electronic burden in its steady obstruction mode was utilized at the MIC yield terminals for the independent case.
3. **DC microgrid:** The MIC was incorporated into a DC microgrid as appeared in Fig. 1. The DC transport voltage Vo was set to 120 V. The DER of Fig. 1 was demonstrated by a DC power

International Journal for Innovative Engineering and Management Research
A Peer Revieved Open Access International Journal
www.ijiemr.org

source. This DER controls the DC transport voltage, and the PVMIC blend goes about as a present source. An electronic heap of fixed obstruction speaks to the microgrid load. Its opposition was set to 60 Ω. The DC transport voltage, MIC yield current and control, and the DER yield power were recorded. The exploratory arrangement is delineated in Fig. 8c.

4. **MIC control for SFM and MPPT:** The control calculation was customized on the microcontroller chip PIC16F877A. The microcontroller least obligation proportion venture of 0.4 % is utilized for precise MPP following and for diminishing the impact of breaking point cycle swaying. Point of confinement cycle swaying brings about low recurrence sounds in the converter yield voltage because of the motions of the obligation proportion around its ideal worth. The parameters of the SFM plan are given in Table I.

5. Resonance issues when changing the MIC topology are kept away from by deactivating the PWM flag through the MIC control for a brief span interim of two inspecting periods. Likewise, imminent resonances are handled by: utilizing exchanging frequencies a lot higher than any potential reverberation recurrence, having damping activity through the parasitic resistors, and by the executed hysteresis impact.

6. MIC sub-circuits: The MIC sub-circuits perform the following functions:

Gate driving: The chip TC4427 is utilized for molding the PWM signal from the microcontroller. One of the two PWM flag in the interleaved case is exposed to a stage move, and afterward the two sign are molded by the chip.

Phase shifting: The stage moving of the PWM signal for the interleaved converter cell is cultivated utilizing the chip LTC6994-2. As indicated by (26) of Appendix C, five phases of the chip with single obstruction RSET equivalent to 250 kω are utilized to stay away from heartbeat skipping and the comparing subharmonics.

Representing irradiance level: The degree of the irradiance is spoken to by a voltage signal from a potentiometer and is sustained to the microcontroller. A physical irradiance estimation gadget in addition to a molding circuit might be utilized, on the other hand. For indoor research center testing and climate free situations, the methodology utilizing the potentiometer is liked.

Measuring: The estimation of the PV module current was finished with the chip INA168 utilizing a 20 mω sense resistor and a detecting increase of 40. The power misfortune in the sense resistor, the exactness of estimation, and the sign molding for the microcontroller were the reason for deciding the size of the sense resistor. The module voltage was acquired through a potential divider, a channel, and an operational enhancer OPA340 to dodge the stacking impact.

B. PERFORMANCE RESULTS

In this subsection, the framework execution results are introduced. This is explored through the estimations of: MIC yield control, yield swell, EMI, control misfortunes, and framework effectiveness. For the MIC yield power and yield swell examinations, the independent case was researched trailed by the DC smaller scale matrix case. For the EMI test, just the independent case was considered to dodge EMI impact from other miniaturized scale network components. The power misfortunes and framework productivity were estimated independently for the independent and DC microgrid cases. At that point, those estimations were arrived at the midpoint of for result portrayal.

International Journal for Innovative Engineering and Management Research
A Peer Revieved Open Access International Journal
www.ijiemr.org

1) Output power: The converter yield power was estimated for a stepwise evolving irradiance. The irradiance level and the relating exchanging recurrence are plotted together with the module yield control in Fig. 9a for the independent case. The test results intently coordinate the recreation aftereffects of Fig. 7a.

For the microgrid case and under a similar irradiance time arrangement of Fig. 9a, the DC transport voltage and the MIC yield

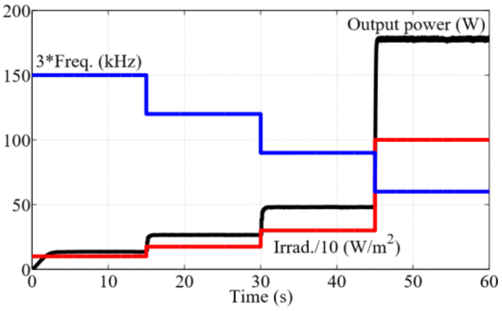

(a)

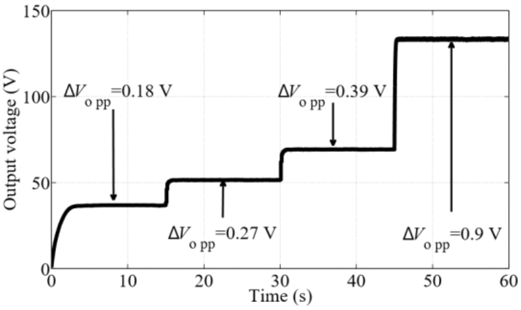

(b)

Fig. 9. Independent case test step evolving irradiance: (a) yield control and the exchanging recurrence; (b) yield voltage and its swell substance.

2) power are portrayed in Fig. 10a. The comparing DER yield power and resistive burden power are appeared in Fig. 10b. The heap intensity of around 240 W was provided by the PV source and DER. In this manner, the DER yield power diminishes with the expansion of provided PV control because of rising irradiance. The MIC had the option to fluctuate the exchanging recurrence dependent on the irradiance, track the most extreme power, and work in CCM.

3) **Output ripple:** The output voltage and its ripple like the irradiance statistic of Fig. 9a ar shown in Fig. 9b for the standalone case. For the four analyzed irradiance segments, values of zero.18 V, 0.27 V, 0.39 V, and 0.9 V were measured for the output voltage ripple, severally. though the change frequency moved from fifty kilocycle to twenty kilocycle, the voltage ripple solely exaggerated from zero.47% at rock bottom irradiance to zero.68% at the very best irradiance. this is often due to the activation of the additional interleaved boost cell at twenty kilocycle once the irradiance is high. The yield voltage and its swell relating to the irradiance time arrangement of Fig.9a are appeared in Fig.9b forthe independent case. For thefour examined irradiance sections, estimations of 0.18V,0.27V,0.39V, and 0.9Vwere estimated forthe yield voltage swell, separately. Despite the fact that the exchanging recurrence movedfrom 50 kHz to 20 kHz, the voltage swell just expanded from 0.47% atthe most minimal irradiance to 0.68% at the most noteworthy irradiance. Thisis on account of the enactment of the extrainterleaved lift cell at 20 kHz when theirradiance is high.

TheMIC yield currentinthe DC microgrid case is appeared in Fig. 10c. The crest to crest yield current swell at thefour irradiance fragments was observed tobe 4 mA, 9mA, 17mA, and 59mA, individually. In mean time, the DC transport voltage had a swell substance of 0.3%. Concerning thevoltage swell in the independent case, the ascent ofthe present swell with diminishing exchanging recurrence is additionally limited through the enactment ofthe interleaved lift cell in the DC microgridcase.

International Journal for Innovative Engineering and Management Research
A Peer Revieved Open Access International Journal
www.ijiemr.org

4) EMI: The emanated EMI ofthe most noteworthy irradiance of 1 kW/m2 was broke down speaking to the most dire outcome imaginable of most elevated info control. Atthis working point, theSFM gives an exchanging recurrence of 20 kHz. The outcomes got

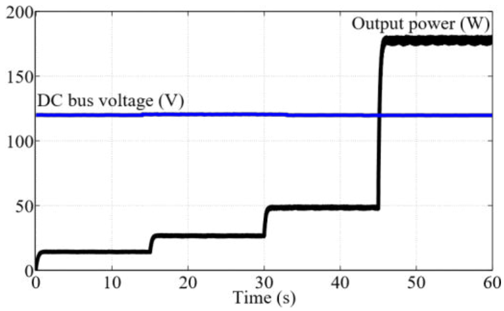

(a)

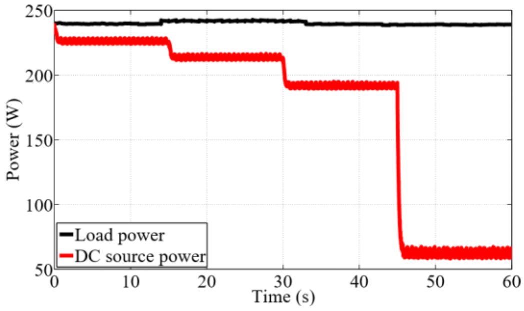

(b)

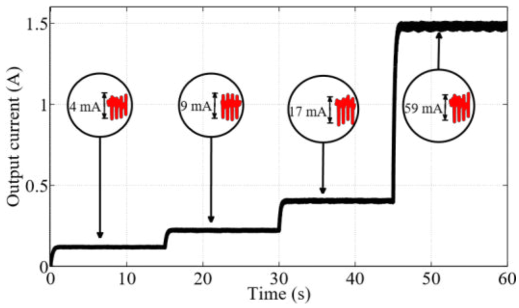

(c)

Fig. 10. DC microgridcase experimental step changingirradiance: (a) MICoutput power and the DCbusvoltage; (b) load and DER power; (c) MICoutputcurrent and its ripplecontent.

proposedMIC are appeared inthe upper diagram ofFig.11. With the end goal of correlation, the interleaved cellof theMIC wasthen deactivated for a subsequent investigation. The relating EMI range is appeared inthe lower chart of Fig. 11. With theinterleaved cell dynamic, theEMI was diminished by around 15 dBmV. The deviationfrom a perfect range is credited to the ceaseless variety of D due toMPPT and thenon uniform stage moving brought about by deferrals of the switches, door drivers, or stage moving circuits. The job ofthe interleaved convertercell in decreasing EMI is steady withthe perceptions of [24], [26].

5) **Power losses:** The general power misfortunes of theMIC incorporate the misfortune in following theMPP, theMIC conduction and exchanging influence misfortunes, the estimation misfortune, and the influence required forthe control circuit. The effectiveness in following theMPP was constantly above 98.5%, keepingthe MPPT misfortunes beneath 1.5 % as indicated by the readings onthe Agilent E4361A. The power change proficiency was demonstrated tobe about 98%,

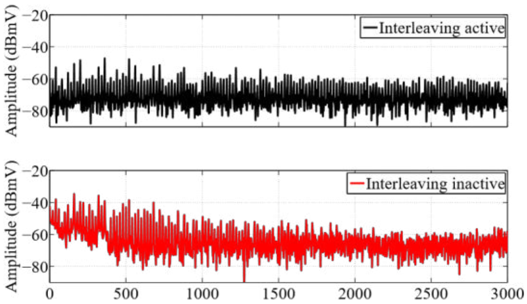

Frequency (kHz)

Fig. 11. MIC EMI spectrumat 1 kW/m^2 and f_s=20 kHz withandwithout the interleaved MICcell under identicaloperating conditions.

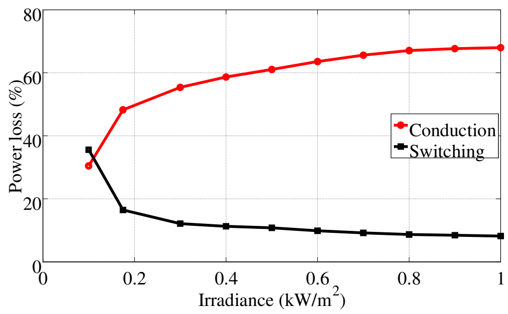

Fig. 12. MIC conductionand switching lossesat different irradiancelevels relative totheoverall powerloss.

International Journal for Innovative Engineering and Management Research
A Peer Revieved Open Access International Journal
www.ijiemr.org

giving an all out power change lossof around 2 %. The controlcircuit control utilization is around 1 W.

The MIC conductionand changing force misfortunes in respect to the general influence misfortunes at various irradiances are appeared inFig.12. Atlow irradiance, the exchanging misfortunes are higherthan conduction misfortunes because of thehigh exchanging recurrence and low PV current. the commitment ofthe conduction misfortunes to the all out misfortune is a lot higherthan for exchanging misfortunes.

5) System efficiency: The general framework proficiency at various irradiance levelswas assessed in respect toother PWM plans. The proposed versatile SFM conspire with and without theinterleaved MICcell was contrasted and twofixed recurrence plans of 50 kHz as in [3] and 20 kHz as in [6] in discrete examinations. Foreach analysis, the consistent stateMIC yield power partitioned bythe most extreme identifiable PV control every irradiance levelwas registered. The outcomes are appeared inFig.13.

Contrasted and thefixedhigh recurrence plot, the exhibition oftheproposed SFM plan was comparative atlow irradiance. In the two cases, CCMactivity was kept up. At highirradiance, be that as it may, the effectiveness of the proposed plan was higher because of diminished exchanging misfortunes. The proposedSFM plan was then contrasted with the fixedlow recurrence PWM plot. At low irradiance, DCM activity was watched forthefixed low recurrence plot. This brought about less gathered PV control. In this way, less effectiveness was acquired contrasted and the proposed SFM conspire. Just athigh irradiance, the presentation of low recurrence

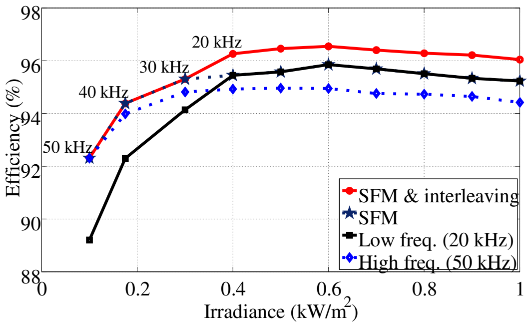

Fig. 13. Average overalLefficiency at differen irradiance levelsforthe proposed scheme in comparison totwofixed switchingfrequencyschemes.

what's more, proposedSFM plans was indistinguishable. Withthe actuation of an interleaved MICcell, notwithstanding, a proficiency addition was not out of the ordinary. The examination affirmed an expansion of proficiency of the request for 0.5 % for this case. Somewhat decreased efficiencies of 92.5% and 94.3% were found for the irradiance levels of 0.1 kW/m2 and 0.175 kW/m2 because of higher exchanging misfortunes. The tests so affirmed the superior of the proposedMIC at all irradiancelevels forboth proficiency and powerquality.

VI. CONCLUSIONS

An epic PVmodule coordinated converter (MIC) reasonable for boostingvoltages for DC independent and DCmicrogrid applicationswas structured, executed, and tried. Theproposed exchanging recurrence regulation chooses anirradiance adjusted exchanging recurrence thatis in every case sufficiently high to stay away from activity in broken conductionmode. Ata high irradiance, the exchanging recurrence tweak setsa lower an incentive for the recurrence, guided bythe take a stab at high productivity through low exchanging misfortunes. The proposed mechanized strategy has demonstrated to be successful in scanning forthe ideal number and benefits of exchanging frequencies. Moreover, aninterleaved lift cell is initiated at high irradiance to hold an abnormal state of intensity quality. Hysteresis capacities bolster the advances between various discrete exchanging frequencies asthe irradiance changes. The versatile MICcontrol plan is supplemented by a MPPT intended for optimizing. Consequently, by consolidating the SFM with the versatile use of the lift converter interleaved cellsanda quick MPPT, focuses of productivity and powerquality are come to.

The effectiveness forthe whole MIC including allpower transformation and control capacities estimated ataround 95% or higher forirradiance levels going from 0.3 kW/m2 to 1.0 kW/m2. The voltage swell stayed underneath 0.7% during testing.The model was evaluated at 400 W to make the structure appropriate for coordinating photovoltaics in DC microgridsor sunlight-based homes. Circulated most extreme powerpoint following is certainly bolstered throughthemodule reconciliation.

REFERENCES

1. REN21.2016, “Renewables 2016 Global Status Report,” RenewableEnergy Policy Network for the 21st Century, Paris,Tech.Rep., 2016.
2. E.Romero-Cadaval,G.Spagnuolo,L.G. Franquelo,C-AndresRamos-´Paja,T. Suntio,andW-MichaelXiao, “Grid-Connected Photovoltaic Generation Plants: Components and Operation,” IEEE Ind. Electron.Mag.Vol.7,no.3,pp. 6–20,Sep.2013.
3. M.DasandV.Agarwal, “Design and Analysis of a High-Efficiency DCDC Converter With Soft Switching Capability for Renewable Energy Applications Requiring High Voltage Gain,” IEEETrans.Ind.Electron., vol.63, no.5,pp.2936–2944,May2016.
4. F.Wang, F.Zhuo,F.C.Lee,T.Zhu,andH. Yi,“Analysis of ExistenceJudging Criteria for Optimal Power Regions in DMPPT PV Systems,” IEEETransEnergy Convers., vol.31,no. 4,pp.1433–1441,Dec.2016.
5. O.Khan,W.XiaoandM.S.E.Moursi, “A New PV System Configuration Based on Submodule Integrated Converters,” IEEETrans. PowerElectron., vol.32, no5, pp3278–3284, May2017.
6. F.Wang,T.Zhu,F.Zhuo,H.Yi,S.ShiandX. Zhang, “Analysis and Optimization of Flexible MCPT Strategy in Submodule PV Application,” IEEETrans. Sustain. Energy, vol.8,no.1,pp.249–257,Jan. 2017.
7. M.A.G.deBrito,L.Galotto,L.P.Sampaio, G.d.A.eMelo,andC.A.Canesin, “Evaluation of the Main MPPT Techniques for Photovoltaic Applications,” IEEETrans. Ind.Electron., vol.60,no.3,pp.1156–1167, Mar.2013.

8. F.F.Edwin,W.Xiao,V.Khadkikar, “Dynamic Modeling and Control of Interleaved Flyback Module-Integrated Converter for PV Power Applications,” IEEETrans. Ind.Electron., vol.61,no.3, pp. 1377–1388,Mar.2014.
9. M.S.S.Andrade,L.Schuch,andM.L.da SilvaMartins, “High Step-Up PV Module Integrated Converter for PV Energy Harvest in FREEDM Systems,” IEEETrans. IndAppl., vol53no.2,pp. 1138– 1148, Mar.2017.
10. C.T.Pan,M.C.Cheng,C.M.Lai,andP.Y.C hen, “Current-RippleFree Module Integrated Converter With More Precise Maximum Power Tracking Control for PV Energy Harvesting,” IEEETrans. Ind. Appl.